

Frequency stability of a dual-mode whispering gallery mode optical reference cavity

L.M. Baumgartel^{1,2}, R.J. Thompson¹, and N. Yu^{1,*}

¹Jet Propulsion Laboratory, California Institute of Technology, 4800 Oak Grove Dr, Pasadena 91109, California, USA

²Department of Physics and Astronomy, University of Southern California, Los Angeles 90089, California, USA

*Corresponding Author: nan.yu@jpl.nasa.gov

Abstract

We report an investigation of laser frequency stabilization using a whispering gallery mode resonator that is temperature stabilized by a dual-mode technique. This dual-mode technique has yielded mode volume temperature instabilities at the nK level, suggesting that high frequency stability may also be reached. Here, we experimentally and theoretically investigate the dynamics of such a system and the important factors affecting the achievable frequency stability. We calculate that the dual-mode technique can reduce the effective fractional temperature coefficient of the reference system to $3.5 \times 10^{-8} \text{ K}^{-1}$ within the temperature feedback bandwidth. We demonstrate a laser stabilized to 1.3×10^{-12} at one second and a linear drift of 21 kHz/hr.

1 Introduction

Whispering gallery mode resonators (WGMRs) demonstrate extremely high quality factor and correspondingly narrow linewidth optical resonances over a large wavelength range, making them attractive for laser frequency stabilization applications. In fluoride resonators, quality factor (Q) in excess of one billion is regularly demonstrated, and $Q > 6 \times 10^{10}$ has been achieved [1], corresponding to a linewidth of ≈ 4.5 kHz – comparable to that of high-finesse Fabry Pérot (FP) cavities. The wide transparency window mitigates the need for expensive mirror-coating runs and facilitates use of a single cavity at multiple wavelengths, while their compact size and robustness to mechanical vibrations makes them well suited for applications requiring portable high-performance lasers.

Impressive gains to laser linewidths and short-term stability have already been achieved using WGMRs. Linewidths of 13 kHz were demonstrated with a resonator acting as a transmission filter in a fiber laser cavity [2], and a 200 Hz linewidth was achieved through injection locking to a WGMR [3]. When employed as an external frequency reference cavity, crystalline resonators have delivered Allan deviations of 6×10^{-14} at 100 ms [4].

Frequency stability of WGMR reference cavities is limited by the fact that, in contrast to an FP resonator, the light travels in a solid medium. At short time scales, thermorefractive noise defines the limit and has been analyzed theoretically [5, 6] and measured experimentally [7]. At longer time scales, stability is limited by temperature changes in and around the resonator. These changes pull the frequency both through thermorefraction and thermal expansion, though the latter tends to be dominant in optical crystals. Ultra-low expansion (ULE) glasses have thermal expansion coefficients about three orders of magnitude lower than common optical

crystals, but their poor transmission qualities preclude their use as a WGMR material.

Recently, dual-mode temperature stabilization schemes have been investigated as a means to address this heavy dependence of frequency on temperature [8–11]. In such schemes, the frequency spacing between modes with different temperature coefficients of frequency (tempcos) provides an extremely sensitive measurement of the mode volume temperature and facilitates active stabilization thereof. Mode volume temperature instabilities less than 10 nK have been demonstrated [8, 9]. But the WGMR represents a complex thermal system with several different sources, sinks and the resulting gradients. We find that a highly stabilized mode volume temperature does not guarantee frequency stability, a finding also suggested by other recent work [10].

Here, we investigate through experiments and numerical modeling how various heat sources affect the temperature distribution in the resonator. By measuring the locked laser’s frequency change as a function of various thermal parameters, we gain an understanding of the mechanisms limiting performance and the steps necessary for their mitigation. In particular, we find that the dual-mode technique leads to unstable temperature gradients in the resonator that pull the frequency through thermal strain. Despite these limitations, the technique reduces the effective temperature coefficient of the WGMR reference cavity by more than an order-of-magnitude, and we achieve an optical frequency instability of 1.3×10^{-12} at one second and a linear drift of 21 kHz/hr.

2 Dual-mode Stabilization

As described in detail previously [8], the thermorefractive coefficients of orthogonally polarized modes in a birefringent resonator are significantly different. Therefore, the frequency spacing between ordinary and extraordinary modes depends heavily upon temperature. The dependence is given by $d(\Delta f)/dT = -f_0(\alpha_n^{(o)} - \alpha_n^{(e)})$, where $\alpha_n^{(o,e)}$ are the thermorefractive coefficients of the ordinary and extraordinary polarizations, and f_0 is the optical carrier frequency. For magnesium fluoride (MgF_2) at our experimental temperature of 40 °C and $f_0 = c/1560$ nm, the differential tempco is 67 MHz/K. With a multi-mode resonator, one can easily identify a pair of modes with spacing in the tens-of-megahertz range. And with the narrow linewidths in a MgF_2 resonator, a frequency spacing measurement on the Hz level is readily achieved, yielding nK sensitivity.

2.1 Experimental Setup

Our implementation of the dual-mode stabilization scheme is shown in Fig. 1 and described as follows. A narrow linewidth fiber laser is coupled via an angle-polished fiber [12] into 3.25 mm diameter, z-cut resonator made from excimer-grade MgF_2 . Mode linewidths are in the range of 40-80 kHz, corresponding to quality factors of $2.4\text{-}4.8 \times 10^9$, depending on the mode order, polarization, and loading conditions. Laser light passes first through an acousto-optic modulator (AOM), and then an electro-optic phase modulator (EOM), before being coupled into the cavity at a polarization angle that can excite both modes. Two modulation frequencies are applied at the EOM: a 1 MHz signal for generation of Pound-Drever-Hall error signals [13], and a second signal at the frequency spacing Δf between a chosen pair of orthogonal modes. Thus, the laser is frequency locked to the ordinary mode, while the modulation sideband coincides with the extraordinary mode, providing an error signal for temperature stabilization. Thermal feedback (unity gain bandwidth ~ 1 Hz) to the resonator is provided by a thermoelectric module (TEM) glued directly to the disc; an optional fast thermal loop actuates on the in-coupled laser intensity via the AOM. The resonator-TEM assembly is mounted in a small brass oven,

ference between resonator and enclosure, q_{rad} is calculated using equation (1) and then applied as a boundary condition on the resonator surface.

Laser light circulating in the mode is converted to heat through material absorption. For a laser locked on resonance (zero detuning), the heat generated by this absorption can be estimated through [15]

$$q_{laser} = I\eta \frac{Q}{Q_{abs}} \quad (2)$$

where I is the input laser power, η is the coupling efficiency, and Q (Q_{abs}) are the observed (absorption limited) quality factors. This heat is included in the model as a volume heat source (units of J/m³) applied to the region shown in pink in Fig. 2(a).

Heat generated in the TEM (q_{TEM}) is modeled as a volume source distributed over the top alumina plate. The bottom of the TEM is held at the enclosure temperature. Thus, we can model how the three heat sources q_{rad} , q_{laser} , and q_{TEM} contribute to the mode volume temperature. A steady-state solution is found assuming reasonable values of in-coupled laser power, with $q_{TEM} = q_{rad} = 0$, yielding initial values of disc radius and mode volume temperature. The dual mode condition is simulated by demanding that subsequent changes in q_{rad} or q_{laser} are compensated for by a change in q_{TEM} , maintaining the mode volume temperature at its initial value. The resulting strains (changes in radius) are converted to frequency, allowing us to model how a change in enclosure temperature or laser intensity that occurs while the dual-mode loops are closed will affect the frequency of the resonator.

3 Results

The dual-mode scheme measures and stabilizes the temperature in the region occupied by the two modes. Our loop guarantees that any uncontrolled (out-of-loop) change in thermal transport parameters will result in a compensating change in the level of thermal feedback actuation. As the relative strengths of these thermal parameters changes, the system moves along lines of constant mode volume temperature. These isotherms do not, however, represent lines of constant resonance frequency because the central portion of the resonator changes temperature and expands/contracts. The isotherm slope, i.e., the ratio of change in optical frequency to the change in a thermal parameter, represents an effective coefficient of frequency.

3.1 Environmental Temperature Dependence

The actively stabilized system can be considered as a system with reduced sensitivity to environmental temperature fluctuations. We simulated the dual-mode resonator's effective tempco by solving the FEM model for various temperature differences between resonator and enclosure (T_1 and T_2 in equation (1)). The condition $T_1 = T_2$ means the average resonator temperature is in equilibrium with the oven and represents the instant at which the dual-mode loops are closed. This $q_{rad} = 0$ situation is solved first. Next, a small drift in T_2 is imposed, q_{rad} is calculated, applied as a boundary condition on the resonator, and the necessary value of q_{TEM} needed to return the mode-volume temperature to its initial value is found (this represents the feedback action of the dual-mode loop).

The result is illustrated in Fig. 2, where the different thermal distribution resulting from a change in enclosure temperature is clearly visible. At $T_2 = T_1$, no radiative heating of the disc occurs; the gradient forms as optically-generated heat is conducted out through the TEM. If the oven temperature drifts up by 50 mK, radiation additionally heats the top and outer portion of the disc. Maintaining the mode volume temperature – out to the nK digit in these simulations – requires that the TEM cool the central-bottom portion of the resonator, contracting it

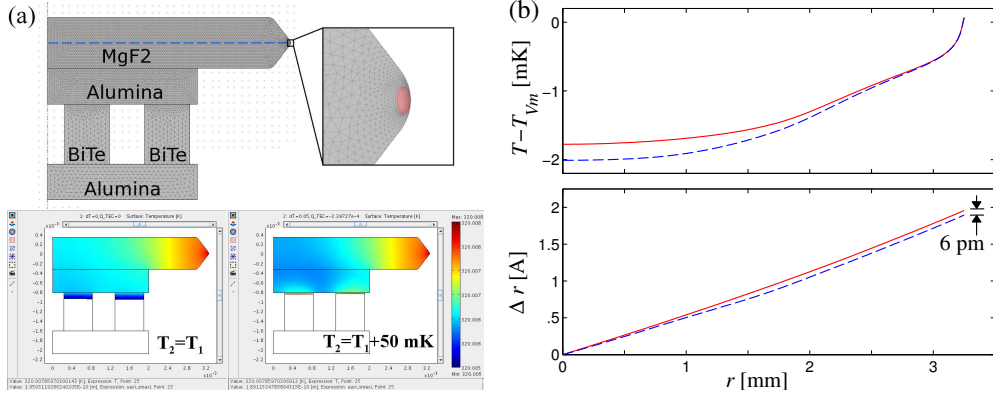


Figure 2: FEM simulation. Screenshots (a) showing: (top) the model setup and meshing, a detail of the mode volume, and the line along which temperature and strain are plotted. BiTe: bismuth telluride; (bottom) Temperature maps showing how different gradients exist for different relative strengths of heat sources. Plots (b) of temperature and radial deformation along the disc radius for $T_2 = T_1$ (solid red) and $T_2 = T_1 + 50 \text{ mK}$ (dashed blue), showing how the latter distribution is cooler in the center, contracting the disc radius by $\approx 6 \text{ pm}$.

and increasing the common-mode optical frequency. The plots in Fig. 2(b) show the calculated distribution of temperature and deformation along a radial line (dashed blue in Fig. 2(a)). The temperature distribution is normalized to the mode volume temperature (T_{Vm}), and the difference in strains at the endpoint ($R = 3.25 \text{ mm}$) yields the frequency shift. The calculated shift was found to be linear across five values of oven temperature drift spanning half a degree. A linear fit to these simulated data yield an effective tempco of 6.9 kHz/mK . We note that this value is comparable to the specified linear thermal expansion coefficients of common ULE glasses.

The effective tempco was also measured experimentally. With the dual mode stabilization loops engaged, we increased the setpoint on the oven’s digital temperature controller in 12 mK steps every 360 seconds (eventually returning it to its initial value). The TEM current (converted to heat via values on the TEM’s datasheet), locked laser’s optical frequency, and in-loop temperature error signal were simultaneously recorded during the run, and are presented in Fig. 3. In agreement with the simulation, increased radiative heating of the disc results in compensatory cooling from the TEM, leaving the mode volume temperature the same but the optical frequency higher. A linear fit of the optical frequency as a function of change in enclosure temperature gives an effective tempco, with the experimental value being 25.5 kHz/mK . The value is 67 times less than the thermal-expansion coefficient of 1.7 GHz/K for MgF_2 .

3.2 Laser Power Dependence

Despite MgF_2 ’s extremely high transmission at 1560 nm , absorbed optical power is constantly converted to heat in the mode volume. Thus, changes in circulating optical power will destabilize the optical frequency at any time scale. Here, we investigate the effect of slow (within the TEM loop bandwidth) circulating power changes. These slower changes may be harder to control since they result from drifts in polarization or coupling strength, while faster fluctuations are in principle corrected for by the intensity dual-mode loop. Similar to the case of environmental temperature, we find a multi-parameter dynamic whereby a change in circulating power results in a change in TEM correction signal, thermal gradient, and resonator frequency.

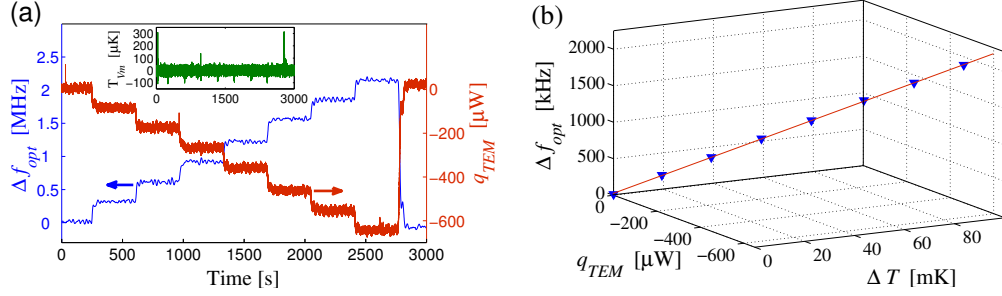


Figure 3: Effect of enclosure temperature: Time series (a) showing shift in optical frequency (Δf_{opt}) and heat delivered to the resonator by the TEM as enclosure temperature changes. Inset shows mode volume temperature from the in-loop error signal; aside from spikes at the temperature steps, it remains extremely stable. The isotherm (b) from fits to the data shows the multi-dimensional relationship between parameters.

Using the same FEM model described above, we calculated the frequency shift as a function of change in circulating optical power. For these simulations q_{rad} was kept at zero. Heat was allowed to leave the resonator radiatively through its surface (to a boundary at infinity) and via conduction through the TEM. For a given change in circulating power, the resulting change in q_{TEM} necessary to maintain the mode volume, change in thermal gradient, and shift in frequency was calculated. Using equation (2) and reasonable values of $I = 100 \mu\text{W}$ at the coupler, $\eta = 0.07$, and that the disc's quality factor is absorption limited, the simulations suggest that a 5% reduction in laser power will yield a frequency shift of -103 kHz.

An experimental measurement of this isotherm slope was also made. With the laser intensity branch of the thermal loop open, we changed the optical power sent to the resonator by varying the amount of light transmitted through the AOM. In agreement with the simulations, a decrease in circulating power causes an increase in TEM heating to maintain the mode volume temperature. The new thermal gradient is warmer in the disc center, increasing r and decreasing the optical frequency. The experimentally measured frequency pulling was -15 kHz for a 5% reduction in intensity, corresponding to an effective coefficient of 43 kHz/ μW of circulating optical power. Based on this result, a stability of ~ 47 pW would be needed to reach a benchmark fractional frequency instability of 10^{-14} . This requirement on laser intensity stabilization is a readily achieved 7 ppm, however we stress that the requirement is on circulating power, so coupling strength and polarization angle (which changes the power ratio between modes) also require ppm-level stability.

The discrepancy between simulated and experimentally determined temperature coefficients results from the heavy dependence on setup details such as boundary conditions at the domain interfaces and values of material properties; assumptions made in using equations (1) and (2) could also lead to errors. Experimentally, it is difficult to isolate a single variable as can be done with simulation, so various other destabilizing factors can play a role. However, the simulations and experiments agree extremely well qualitatively, provide meaningful insight, and with refinement could agree quantitatively as well.

3.3 Dual-mode Frequency Stability

To evaluate the performance gained from the dual-mode temperature stabilization technique, we made optical comparisons to the frequency comb. After the AOM, a portion of the stabilized

laser light was picked off and beat on a photodiode with a bandpass-filtered span of the comb. For several thousand seconds, the beatnote was counted with 10 ms gate times and results of two typical data runs are shown in Fig. 4. The lowest instability of 1.29×10^{-12} was reached at 700 ms, while a linear fit to the time-series frequency excursions yields a drift-rate of 21 kHz/hr.

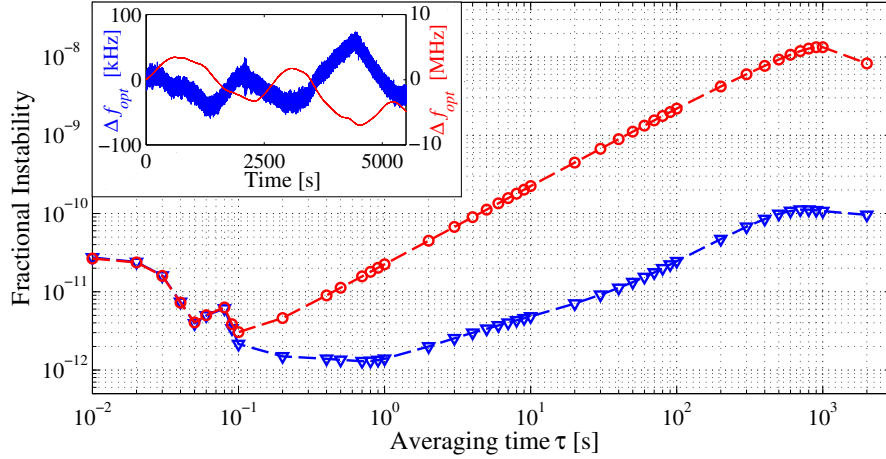


Figure 4: Overlapping Allan deviation of a laser locked to the WGMR. Dual-mode stabilization (blue triangles) yields better performance than the free-running case (red circles) for time scales > 100 ms. Inset: Time sequences of the data run showing changes in the optical frequency for the dual-mode (blue, left scale) and free-running (red, right scale) resonator.

In Fig. 4, we show data for both the dual-mode stabilized and “free-running” resonator, where the later configuration is identical except that the temperature feedback loop is open. The dual-mode stabilization technique provides an improvement factor of 16.1 at one second and 46.4 at ten seconds. Assuming that the bulk temperature of the free-running resonator is in thermal equilibrium with the enclosure, one expects the tempco to be ≈ 1.7 GHz/K (defined by thermal expansion in MgF_2). This value is 67 times greater than the experimentally determined dual-mode enclosure tempco of 25.5 MHz/K, in reasonable agreement with these improvement factors. Temperature fluctuations of the oven – caused by oscillations of the analog control loop and room fluctuations – remain the overall limit to stability performance. The effective dual-mode tempco is about an order of magnitude larger than that of ULE cavities, and although our efforts to stabilize the environmental temperature are modest, the average drift rate of 21 kHz/hr is to our knowledge the best long-term stability of a whispering gallery mode resonator.

4 Conclusion

We have investigated the frequency stability of a laser locked to a dual-mode WGMR reference cavity. Because the temperature distribution in the resonator depends on several thermal parameters simultaneously, we find that a precisely stabilized mode volume temperature does not guarantee corresponding frequency stability. Nonetheless, we calculate that the dual mode technique can reduce the temperature coefficient to $3.5 \times 10^{-8} \text{ K}^{-1}$, comparable to the linear coefficient of ULE. In addition to environmental temperature, the level of circulating optical power also plays a significant roll. We experimentally demonstrate a reduction of temperature coefficient to $1.7 \times 10^{-7} \text{ K}^{-1}$, a frequency instability at one second of 1.3×10^{-12} , and a drift of

21 kHz/hr over long time periods. These results represent progress towards using WGMRs as optical frequency references for time and metrology applications.

Acknowledgements

This work was carried out at Jet Propulsion Laboratory, California Institute of Technology, under contract from NASA. The authors thank D. Strekalov, I.S. Grudin, and D. Aveline for discussions and contributions to the experimental setup.

References

- [1] I. S. Grudin, V. S. Ilchenko, and L. Maleki, “Ultra-high optical Q factors of crystalline resonators in the linear regime,” *Phys. Rev. A* **74**, 063806 (2006).
- [2] B. Sprenger, H. G. L. Schwefel, Z. H. Lu, S. Svitlov, and L. J. Wang, “CaF₂ whispering-gallery-mode-resonator stabilized-narrow-linewidth laser,” *Opt. Lett.* **35**, 2870–2872 (2010).
- [3] W. Liang, V. S. Ilchenko, A. A. Savchenkov, A. B. Matsko, D. Seidel, and L. Maleki, “Whispering-gallery-mode-resonator-based ultranarrow linewidth external-cavity semiconductor laser,” *Opt. Lett.* **35**, 2822–2824 (2010).
- [4] J. Alnis, A. Schliesser, C. Y. Wang, J. Hofer, T. J. Kippenberg, and T. W. Hänsch, “Thermal-noise-limited crystalline whispering-gallery-mode resonator for laser stabilization,” *Phys. Rev. A* **84**, 011804 (2011).
- [5] A. A. Savchenkov, A. B. Matsko, V. S. Ilchenko, N. Yu, and L. Maleki, “Whispering-gallery-mode resonators as frequency references. II. stabilization,” *J. Opt. Soc. Am. B* **24**, 2988–2997 (2007).
- [6] A. Chijioko, Q.-F. Chen, A. Y. Nevsky, and S. Schiller, “Thermal noise of whispering-gallery resonators,” *Phys. Rev. A* **85**, 053814 (2012).
- [7] M. L. Gorodetsky and I. S. Grudin, “Fundamental thermal fluctuations in microspheres,” *J. Opt. Soc. Am. B* **21**, 697–705 (2004).
- [8] D. V. Strekalov, R. J. Thompson, L. M. Baumgartel, I. S. Grudin, and N. Yu, “Temperature measurement and stabilization in a birefringent whispering gallery mode resonator,” *Opt. Express* **19**, 14495–14501 (2011).
- [9] L. Baumgartel, R. Thompson, D. Strekalov, I. Grudin, and N. Yu, “Dual mode frequency stabilization of a whispering gallery mode optical reference cavity,” in “CLEO: Science and Innovations,” (Optical Society of America, 2012), p. CTh3A.6.
- [10] I. Fescenko, J. Alnis, A. Schliesser, C. Y. Wang, T. J. Kippenberg, and T. W. Hänsch, “Dual-mode temperature compensation technique for laser stabilization to a crystalline whispering gallery mode resonator,” *Opt. Express* **20**, 19185–19193 (2012).
- [11] P. Del’Haye, S. Papp, and S. Diddams, “An all-optical resonator stabilization scheme with laser machined SiO₂ microresonators,” in “CLEO: Science and Innovations,” (Optical Society of America, 2012), p. CTh3A.7.

- [12] V. S. Ilchenko, X. S. Yao, and L. Maleki, "Pigtailing the high-Q microsphere cavity: a simple fiber coupler for optical whispering-gallery modes," *Opt. Lett.* **24**, 723–725 (1999).
- [13] R. W. P. Drever, J. L. Hall, F. V. Kowalski, J. Hough, G. M. Ford, A. J. Munley, and H. Ward, "Laser phase and frequency stabilization using an optical resonator," *Applied Physics B: Lasers and Optics* **31**, 97–105 (1983). 10.1007/BF00702605.
- [14] E. Schmidt, *Thermodynamics: principles and applications to engineering*, Dover books on physics and mathematical physics (Dover Publications, 1966).
- [15] T. Carmon, L. Yang, and K. Vahala, "Dynamical thermal behavior and thermal self-stability of microcavities," *Opt. Express* **12**, 4742–4750 (2004).